CrossMark

ORIGINAL PAPER

BP-1T, an antiangiogenic benzophenone-thiazole pharmacophore, counteracts HIF-1 signalling through p53/MDM2-mediated HIF-1α proteasomal degradation

Prabhu Thirusangu[1] · V. Vigneshwaran[1] · T. Prashanth[2] · B. R. Vijay Avin[1,3] ·
Vikas H. Malojirao[1] · H. Rakesh[1] · Shaukath Ara Khanum[2] · Riaz Mahmood[4] ·
B. T. Prabhakar[1]

Abstract Hypoxia is a feature of all solid tumours, contributing to tumour progression. Activation of HIF-1α plays a critical role in promoting tumour angiogenesis and metastasis. Since its expression is positively correlated with poor prognosis for cancer patients, HIF-1α is one of the most convincing anticancer targets. BP-1T is a novel antiproliferative agent with promising antiangiogenic effects. In the present study, the molecular mechanism underlying cytotoxic/antiangiogenic effects of BP-1T on tumour/non-tumour angiogenesis was evaluated. Evidences show that BP-1T exhibits potent cytotoxicity with prolonged activity and effectively regressed neovessel formation both in reliable non-tumour and tumour angiogenic models. The expression of $CoCl_2$-induced HIF-1α was inhibited by BP-1T in various p53 (WT)-expressing cancer cells, including A549, MCF-7 and DLA, but not in mutant p53-expressing SCC-9 cells. Mechanistically, BP-1T mediates the HIF-1α proteasomal degradation by activating p53/MDM2 pathway and thereby downregulated HIF-1α-dependent angiogenic genes such as VEGF-A, Flt-1, MMP-2 and MMP-9 under hypoxic condition of in vitro and in vivo solid tumour, eventually leading to abolition of migration and invasion. Based on these observations, we conclude that BP-1T acts on HIF-1α degradation through p53/MDM2 proteasome pathway.

Keywords BP-1T · HIF-1α · p53 · MDM2 · Solid tumour · Antiangiogenesis

✉ B. T. Prabhakar
pbtssc@gmail.com

1 Molecular Biomedicine Laboratory, Postgraduate Department of Studies and Research in Biotechnology, Sahyadri Science College (Autonomous), Kuvempu University, Shivamogga, Karnataka 577203, India

2 Department of Chemistry, Yuvaraja's College (Autonomous), University of Mysore, Mysore, Karnataka 570 005, India

3 Department of Pharmacology, Center for Lung and Vascular Biology, University of Illinois at Chicago, Chicago, IL, USA

4 Postgraduate Department of Studies and Research in Biotechnology and Bioinformatics, Kuvempu University, Shankaraghatta, Shivamogga, Karnataka 577203, India

Introduction

The hypoxic microenvironment occurs in tumours, which is most frequently due to the oxygen deprivation and tumour outgrowing the existing vasculature. Cancer cells recognize this microenvironment as an important module to promote angiogenesis, cell proliferation and invasive metastasis [1, 2]. The key molecule expressed under hypoxia is hypoxia-inducible factor-1 (HIF-1), a heterodimeric transcription factor, that consists of the oxygen-sensitive HIF-1α subunit and constitutively expressed HIF-1β subunit [3–5]. Under normoxia, HIF-1α protein is rapidly degraded by protein Von Hippel Lindau (pVHL)-mediated ubiquitin-proteasome pathway, whereas hypoxia blocks this degradation leading to nuclear accumulation of HIF-1α, which induces the expression of many genes including vascular endothelial growth factor (VEGF), fms-related tyrosine kinase 1 (Flt-1), foetal liver kinase 1(Flk-1), matrix metalloproteinase (MMPs) which are predominantly involved in neovessel formation and metastasis [6–8].

HIF-1α is overexpressed in many solid tumours which includes breast, lung, ovarian, pancreatic, prostate, renal

carcinomas, etc., where pVHL is mutated or silenced [5, 6]. Inactivation of pVHL pathway results in upregulation and nuclear accumulation of HIF-1α. Alternatively, HIF-1α ubiquitination and stability is regulated by tumour suppressor proteins p53 and E3 ubiquitin ligase murine double minute 2 (MDM2) [9, 10]. This collection of facts explains the ineffectiveness of targeting pVHL-dependent pathway and urges to target the alternative pVHL-independent p53/MDM2 pathway for proteasomal degradation of HIF-1α. Recently, the molecular interaction among HIF-1α, p53 and MDM2 has been well studied and it has been suggested that p53 acts as a molecular chaperone that facilitates recruitment of HIF-1α for ubiquitination by MDM2 under hypoxic conditions in a proteasome-dependent manner [11–14]. Moreover, MDM2 expression can significantly enhance the interaction between p53 and HIF-1α, indicating that MDM2 may act as a bridge and mediate the indirect interaction between HIF-1α and p53 in tumour hypoxia [15] suggesting both p53 and MDM2 act as a potent negative regulator for HIF-1α protein. These studies open the new gateway to overcome the HIF-1α accumulation through the activation of p53/MDM2-mediated proteasome pathway.

Benzophenones are well known for their potent pharmacological activity including antitumour potentials. Considering benzophenone as parental skeleton, various active analogues were synthesized targeting angiogenic signalling [16–20]. Efforts have been made to improve the potentiality of the molecule based on structure activity relationship to identify gene specific targets. One such target, benzophenone coupled with thiazole moiety, BP-1T (2-[4-(4-fluoro-benzoyl)-2-methyl-phenoxy]-N-[4-(4-methoxy-phenyl)-thiazol-2-yl]-acetamide) with the methyl group in the phenoxy ring, fluoro group in the benzoyl ring and methoxy group in the phenyl ring in thiazole (Fig. 1a) has turned out to have cytotoxicity of IC$_{50}$ ∼ 5 μM against murine cancer cells. It is known to target angiogenic signalling by downregulating VEGF [21]. In the current investigation, the molecular mechanism underlying inhibition of VEGF gene expression was investigated and here we reporting that BP-1T effectively targets p53/MDM2 pathway for HIF-1 proteasomal degradation which reflecting in modulation of HIF-1α transcribed gene expression, eventually leading to improving the pathophysiology of the solid tumour.

Materials and methods

Materials

Cobalt chloride (CoCl$_2$), 3-(4,5-dimethylthiazole-2-yl)-2,5-diphenyltetrazolium bromide (MTT), TRI reagent, sodium bicarbonate (NaHCO$_3$), extracellular matrix (ECM) gel, hydron polymer (poly-hydroxyethyl-methacrylate (poly HEMA), primers, Annexin-V-FITC apoptosis detection kit, propidium iodide (PI), Anti-VEGF-A and anti mouse/rabbit IgG antibodies, protease inhibitor cocktail, human umbilical vascular endothelial cells (HUVEC), endothelial cell growth media (EGM) were obtained from Sigma Aldrich, USA. Anti-HIF-1α, anti-flt-1, anti-MMP-2 and MMP-9, and anti-MDM2 antibodies, p53-siRNA and transfection kit were obtained from Santa Cruz, USA. Anti-p53, anti-β-actin and anti-lamin B from BD bioscience, USA. RNA isolation kit from Zymo research (Epigenetics), USA, Superscript first strand synthesis and PCR supermix for semi-quantitative (RT)-PCR, DMEM medium, antibiotic-antimycotic solution, foetal bovine serum (FBS) were obtained from Invitrogen, USA. Anti CD-31 antibody, immunostaining kit from Leica Biosystems, Germany. All the other chemicals used were of analytical grade. All the photographs were taken using Canon power shot Sx500 IS camera, and all angiogenesis assay results were assessed by ImageJ software.

Cell culture and in vitro treatment

The A549, MCF-7 and SCC-9 cells were cultured, and cytotoxic effect of BP-1T was tested using trypan blue dye exclusion, MTT assay and lactate dehydrogenase (LDH) release assay as described earlier and IC$_{50}$ values were calculated. In brief, the cells were grown in DMEM medium, supplemented with 10 % FBS, antibiotic-micotics and NaHCO$_3$ (0.37 %) and incubated at 37 °C in 5 % CO$_2$, with 98 % humidity. The cells were treated using increasing concentrations of BP-1T (0, 2, 5, 10, 25, 50 μM in DMSO) for 48 h, and each experiment was repeated a minimum of 3 independent times [17, 21].

Hypoxic condition, treatment and cell lysate preparations

A549, MCF-7, SCC-9 and DLA cells were cultured and exposed with CoCl$_2$ (100 μM) to mimic hypoxia and then treated with BP-1T at the concentration of 0, 3, 5 μM for 48 h. RNA was isolated as per manufacturer instructions from A549 cells, and whole-cell lysates from all cell lines were prepared using RIPA buffer (100 mM Tris pH-7.5, 1 % Triton X-100, 0.1 % SDS, 140 mM NaCl, 0.5 % sodium deoxycholate, 5 mM EDTA, 0.5 mM phenylmethylsulfonyl fluoride (PMSF) and protease inhibitor cocktail) [22].

A549 cells were cultured, exposed to plus or minus CoCl$_2$ (100 μM), treated with BP-1T (0, 3, 5 μM) in plus or minus MG132 (10 μM, 26 S proteasome inhibitor for 2 h) or p53-siRNA-transfected cells. Conditioned media
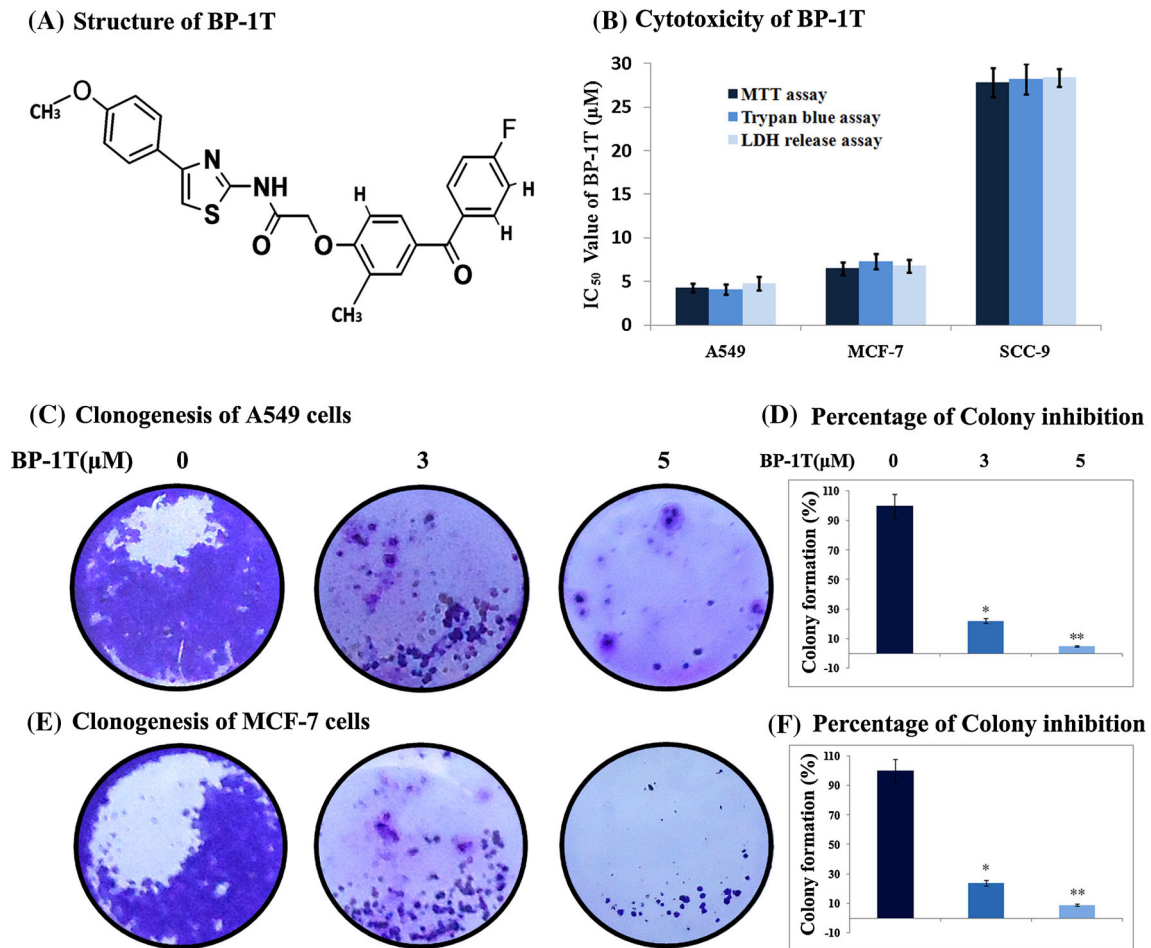
(A) Structure of BP-1T

(B) Cytotoxicity of BP-1T

(C) Clonogenesis of A549 cells

(D) Percentage of Colony inhibition

(E) Clonogenesis of MCF-7 cells

(F) Percentage of Colony inhibition

Fig. 1 BP-1T exhibits the potent cytotoxicity and prolonged activity. **a** Structure of 2-[4-(4-Fluoro-benzoyl)-2-methyl-phenoxy]-*N*-[4-(4-methoxy-phenyl)-thiazol-2-yl]-acetamide (BP-1T). The cells A549, MCF-7 and SCC-9 cells were cultured and treated with BP-1T at various concentrations (0–50 µM) for 48 h. MTT, Trypan blue dye exclusion and LDH release assays were performed and cytotoxicity values were calculated. **b** BP-1T exhibited effective cytotoxicity:

A549 and MCF-7 cells were pretreated with BP-1T (0, 3 and 5 µM) for 6 h and incubated for the period of 12 days to form colonies. **c** and **e** Pictographical representation of A549 and MCF-7 cell clonogenesis inhibition. **d** and **f** Graphical representation of restraining of colony formation. Statistical significant values were expressed as *$p < 0.05$ and **$p < 0.01$

were used for gelatin zymogram, ELISA and whole-cell lysates for immunoblot analysis. Cytosolic fractions were separated by centrifuging the cells lysed in buffer A (10 mM HEPES, 1.5 mM $MgCl_2$, 10 mM KCl, 0.5 mM DTT, 0.05 % NP40, 0.5 mM PMSF and protease inhibitors) at 14,000 rpm for 1 min, and nuclear fractions were prepared by centrifuging the residual pellets resuspended in buffer B (5 mM HEPES, 1.5 mM $MgCl_2$, 0.2 mM EDTA, 0.5 mM DTT, 26 % glycerol (v/v), 0.5 mM PMSF and protease inhibitors) at 14,000 rpm for 1 min for determining the HIF-1α nuclear translocation [23].

Clonogenic assay

The clonogenic assay has been performed with minor modification for determining the prolonged anti-neoplastic effects of BP-1T against A549, MCF-7 and SCC-9 cell

proliferation in vitro [24]. In brief, the cells were cultured, exposed with BP-1T for 6 h, rinsed with fresh medium and cultured further for 12 days. Colonies were fixed with methanol, stained with crystal violet (0.4 g/L), counted and photographed.

Endothelial cell migration and tube formation assay

The HUVECs were cultured in 96-well plate containing EGM medium to form monolayer, and 1-mm size wounds were made by scratching with a microtip and exposed with recombinant $VEGF_{165}$ ($rVEGF_{165}$) (30 ng/ml) and BP-1T (0, 3, 5 µM) for 48 h. Endothelial cell migrations were photographed at identical locations. The effect of BP-1T on HUVECs migration was analysed by comparing final gap width to initial gap width. ECM gel was polymerized for 30 min at 37 °C for coating 96-well plate. HUVECs

$(2.5 \times 10^5$ cells/ml) suspended in EGM medium was added to each well coated with ECM gel and treated with or without rVEGF$_{165}$ and BP-1T (0, 3, 5 μM) for 24 h. Inhibition of the tube formation and tube lengths were observed under a phase-contrast microscope and photographed. Viability of HUVECs was assessed after exposure with rVEGF$_{165}$ and BP-1T at varying concentrations by MTT assay.

Migration assay

A monolayer of A549 cells were scratched to form a wound and treated with BP-1T (0, 3 and 5 μM), incubated for 48 h, fixed with methanol and stained in crystal violet (0.4 g/L). Randomly chosen fields were photographed at 10× magnification at identical locations using Olympus inverted microscope. Percentage of cell migration was calculated by comparing final gap width to initial gap width [25].

Matrigel transwell invasion assay

The A549 cells (5×10^4) in 0.5 ml of serum-free medium containing BP-1T (0, 3 and 5 μM) were seeded onto top of invasion chamber coated with ECM gel and 0.75 ml of complete medium containing 10 % FBS was added to each well in the lower chamber. Following incubation for 24 h at 37 °C, non-invasive cells were removed from the invasion chamber by wet cotton swab and the cells attached to the lower chamber were fixed with methanol, stained with crystal violet (0.4 g/L) and invaded cells were counted in Olympus inverted microscope at 10× magnification and images were documented [26].

FACS analysis

For the determination of cell proliferation and cell death, A549, A549 (p53 silenced), SCC-9 and MCF-7 cells with CoCl$_2$ and BP-1T (0, 3, 5 μM) for 48 h. The cells were harvested by trypsinization and washed with ice-cold PBS, stained with appropriate dyes using apoptosis detection kit and subjected for FACS analysis, and the cells undergoing apoptosis were analysed by using WinMDI version 2.9 software.

CAM xenograft model

In vivo CAM xenograft model was performed to evaluate angiogenesis with slight modification as described previously [27]. In brief, fertilized eggs were incubated, windows were made on 8th day, and cultured A549 cells $(1 \times 10^6$ cells) suspended in 100 μl of ECM gel/DMEM

(1:1) with rVEGF$_{165}$ and BP-1T (0, 3 and 5 μM) were placed on CAMs. Eggs were reincubated after proper sealing for 6 days. Tumours were separated from CAM, photographed and histological sections were processed for microvessel density (MVD) count.

In vivo and ex vivo CAM assays

The rVEGF$_{165}$ (10 ng/CAM)-induced angiogenesis of in vivo and ex vivo CAMs treated with BP-1T (0, 3, 5 μg/CAM) was performed as reported earlier [18, 28]. Angiogenic modulation of BP-1T was assessed and photographed.

Animals and ethics

Swiss albino mice (27–30 g) and Swiss albino rats (150–155 g) were used throughout the study, were maintained as per CPCSEA guidelines and were reviewed and approved by National College of Pharmacy Ethical Committee, Shimoga, India. (NCP/IAEC/CL/101/05/2012-13).

Rat corneal micropocket assay

The rVEGF$_{165}$ (10 ng/pellet)-induced neovascularization in rat cornea exposed with BP-1T (0, 3, 5 μg/pellet) using formulated poly HEMA into rat corneas was performed as mentioned earlier [29]. Corneal remodelling was photographed, and the number of blood vessels (MVD) was quantified by haematoxylin and eosin (H&E) staining.

Rat aortic ring assay

One- to two-millimetre aortic rings from rat thoracic aortas were isolated in sterile condition and sandwiched between ECM gel in 96-well plate, supplemented with DMEM, 20 % FBS, BP-1T (0, 3 and 5 μM) in plus or minus rVEGF$_{165}$ and incubated for 6 days. Sprouting neovessels from aorta were photographed and counted [30].

Peritoneal angiogenesis

Tumour-induced peritoneal angiogenesis was measured as reported earlier [24]. In brief, ascitic lymphomas were treated with BP-1T (0, 30, 50 mg/kg body weight) for three doses intraperitoneally (ip). On 10th day, tumour-induced neovessel formation of peritoneum lining was opened and documented. Corresponding peritoneum tissue sections were processed for H&E staining. Microvessel density/high power field (MVD/HPF) was manually quantified. Ascites tumour growth parameters including tumour volume, ascites secretion, percentage of tumour inhibition and survivability were noticed [20, 31].

Tumour models and treatment

Solid tumour model was developed by adopting reported procedure with minor modification [20, 32]. In brief, the DLA cells were cultured in peritoneum cavity of mice to develop murine ascites tumour. After tumour establishment, DLA cells were withdrawn from donor mice and re-injected (5×10^6 cells/thigh) into the right thigh of the mice subcutaneously (s.c) to develop DL solid tumour (DLS). Mice were grouped separately ($n = 6$ each group) and administered with BP-1T (0, 30, 50 mg/kg body weight (b.w), i.p for 6 doses) after the onset of visible solid tumour (~ 100 mm^3) on every alternate days. The tumour growth of the mice was monitored, and the tumour volume was measured using vernier caliper. At the end of 35th day (after 6 doses), mice were killed and serum was prepared for VEGF quantification. The tumour tissues were separated and photographed; then, total RNA and whole-cell lysates prepared for reverse transcriptase (RT)-PCR & immunoblot, gelatin zymogram analysis respectively and tumour tissues were fixed with 10 % formaldehyde, processed for H&E staining and immunohistochemistry (IHC) analysis. For survivability, mice bearing DLS tumour of BP-1T (0, 30, 50 mg/kg) treated ($n = 10$ each group) was monitored separately and documented. Livers and Spleens were isolated from BP-1T treated and untreated groups for toxic and histological analysis.

Semi-quantitative (RT)-PCR

Semi-quantitative-PCR was performed by following the manufacturer's recommendation and amplified up to 30 cycles using HIF-1α fwd: 5′-TTCACTGCACGGGCCA-TATT-3′ and rev: 5′-TCCACCTCTTTTGGCAAGCA-3′, VEGF-A fwd: 5′-GGGGTGTCCCATAGGGGTAT-3′ and rev: 5′-CGCCTTGGCTTGTCACATTTT-3′, Flt-1 fwd: 5′-TGGGCAGTCAAGTCCGAATC-3′ and rev: 5′-GTGCA AACTCCCACTTGCTG-3′, and GAPDH fwd: 5′-CGCTC ATGTACCCGCTGTAT-3′ and rev: 5′-TGTCTGCCG GACTCAAAGAC-3′. PCR product was resolved by using 1.2–1.5 % agarose gel and documented by Bio-Rad gel documentation™ XR + imaging system.

Immunohistochemistry (IHC)

The DL tumour tissue sections (5 μm) were deparaffinised, rehydrated and boiled in citrate buffer (pH-6.0) for antigen retrieval. Immunostaining of the tumour sections was performed using Leica Biosystems kit as per the manufacturer's instructions provided for CD31, HIF-1α, p53, MMP-2 and MMP-9 with appropriate negative control [33]. The slides were independently evaluated by two pathologists and photographed.

Immunoblots

Immunoblot analysis was carried out for HIF-1α, p53, MDM2, VEGF, Flt-1, MMP-2 and MMP-9, LaminB and β-actin proteins as mentioned earlier [18, 19].

VEGF-ELISA

The in vitro and in vivo secretion of VEGF levels were quantified by using anti-VEGF antibody by ELISA [19].

Gelatin zymogram

Gelatin zymogram was performed to quantify the MMP-2 and MMP-9 activity. Proteins of conditioned media and whole-cell lysate were resolved in 8 % SDS-PAGE gels containing 0.1 % (w/v) gelatin type A. zymogram was developed [31, 34], and results were documented using Bio-Rad gel documentation™ XR + imaging system.

Statistical analysis

Values were expressed as mean ± standard error (SEM). Statistical significance was evaluated by one-way analysis of variance (ANOVA) followed by Student's t test. Statistical significant values were expressed as *$p < 0.05$ and **$p < 0.01$.

Results

BP-1T exhibits potent cytotoxic activity with long term effect

Antiproliferative effect of BP-1T molecule with IC$_{50}$ value of ~ 5 μM against the murine neoplastic cells such as EAC and DLA has been reported earlier by our group [21]. The cytotoxicity effect of BP-1T against human cancer cell lines was extended to determine IC$_{50}$ values by performing MTT, trypan blue and LDH release assays which inferred cytotoxic values 4.4 ± 0.6, 6.8 ± 0.7 and 28.1 ± 1.4 μM for A549, MCF-7 and SCC-9 cells, respectively (Fig. 1b) (Table 1). Eventual cytotoxic effect resulted in inhibition of colony formation at 3 and 5 μM concentration with 77.8 and 94.2 % for A549 (Fig. 1c, d) and 72.8 and 92.4 % for MCF-7 cells (Fig. 1e, f), respectively, but SCC-9 cells showed less sensitivity to BP-1T on clonogenesis (Supplementary Fig. 1A & B). The reticence in colony formation is due to prolonged cytotoxic effect of BP-1T molecule.

BP-1T inhibits the neovessel formation in non-tumourigenic angiogenesis models

To examine the effect of BP-1T on angiogenesis, specific reliable rVEGF$_{165}$-induced non-tumourigenic angiogenic

Table 1 IC$_{50}$ values of BP-1T against A549, MCF-7 and SCC-9 tabulated based upon MTT, Trypan blue and LDH release assays results

Cell line	IC$_{50}$ value: BP-1T (µM)			IC$_{50}$ value: 5-Fluorouracil (µM)		
	MTT assay	Trypan blue	LDH release assay	MTT assay	Trypan Blue	LDH release assay
A549	4.3 ± 0.4**	4.1 ± 0.5**	4.8 ± 0.7	7.4 ± 0.6*	7.8 ± 0.4	7.3 ± 0.7
MCF-7	6.5 ± 0.7*	7.3 ± 0.8	6.8 ± 0.7*	12.2 ± 0.7*	14.7 ± 0.9	13.5 ± 0.6*
SCC-9	27.8 ± 1.6	28.2 ± 1.7	28.4 ± 1.0	9.4 ± 0.7	8.7 ± 0.9	8.6 ± 0.8

5-Fluorouracil is used a positive control and DMSO is used as a vehicle control which showed very negligible cytotoxicity. Values are indicated in mean ± SE (SEM), and statistically significant values are expressed as * $p < 0.05$ and ** $p < 0.01$

models were used. Neovascularization induced by rVEGF$_{165}$ on CAMs was regressed with 55.6–76.3 % in ex vivo (Fig. 2a, b) and 52.8–78.3 % in in vivo (Fig. 2c, d) by BP-1T without any sign of thrombosis and haemorrhage in concentration-dependent manner. Similar results were observed in rat corneal micropocket assay with decreased sprouting neovasculature with MVD count of 71.2 and 84.4 % in BP-1T treated cornea compared to unexposed. The corneal histology depicted improved corneal gesture after BP-1T treatment (Fig. 2e, h). Additionally, BP-1T proved its efficacy by pruning sprouting neovessels from rat aortic endothelial cells up to 78.3 and 86.7 % decrease of MVD (Fig. 2i, j). Further, BP-1T potentiality validated on human endothelial cells by HUVECs viability, migration and capillary tube formation assays. Result postulates that viability of HUVECs by BP-1T was markedly decreased (Fig. 3a). The HUVECs migration was retarded noticeably with 73–86 % by BP-1T at different concentration (Fig. 3b, c). HUVECs are capable of forming tubes via linking to adjacent cells in ECM gel but BP-1T treatment restricted the capillary tube formation and tube length with irregular cell morphology compared to rVEGF$_{165}$ treated and untreated (Fig. 3d). Tube length and branch number were significantly reduced by BP-1T up to 82.3 and 87.1 % at two different concentrations (Fig. 3e).

BP-1T shows the antiangiogenesis effect in tumourigenic angiogenesis models

To re-evaluate the effect of BP-1T on neovascularization on angiogenesis dependent tumour progression, CAM xenograft was performed by using A549 cells with rVEGF$_{165}$. Results unveil that BP-1T visibly reduced 1.7- and 4.0-fold of tumour progression (Fig. 4a, b) by lessening the rVEGF$_{165}$ induced MVD/HPF with 12.1 ± 2.5 (54.8 %) and 4.1 ± 1.6 (84.9 %) compared to 26.8 ± 4.7 of untreated, in concentration-dependent manner (Fig. 4c, d). Antiangiogenic efficacy of BP-1T reconfirmed with DLA induced peritoneal angiogenesis revealed remarkable decrease in neovessel formation (Fig. 4e, f) with 2.75- and 5.93-fold decrease compared to control on varying concentration (Fig. 4g, h). The CD31 counts further inferred

that BP-1T restricted the MVD/HPF to 13.8 ± 2.1 and 6.4 ± 2.3 in 30 and 50 mg/kg treated sections respectively, as compared to control 38 ± 5.7 (Fig. 4i, j). As a result, angiogenesis-dependent tumour development was inhibited up to 61.4 and 77.8 % with decreased ascites secretion and tumour growth, which eventually leading to significant difference in the survival rate compared to the untreated mice (Supplementary Fig. 2A-D).

BP-1T mediates HIF-1α inhibition by p53/MDM2 proteasomal pathway

To investigate the molecular mechanism underlying inhibition of tumour angiogenesis by BP-1T, hypoxic signalling pathway was evaluated since solid tumour microenvironment has hypoxic condition [35]. As an approach, multiple cancer cells were exposed to CoCl$_2$ to mimic hypoxic environment and treated with BP-1T for HIF-1α expression assessment. Semi-quantitative PCR results exhibit no transcriptional alteration of HIF-1α (Supplementary Fig. 3A) but significantly diminished the translational HIF-1α expression in A549, MCF-7 and DLA cells and not in SCC-9 cells due to mutant p53 gene (Fig. 5a). To check the p53 involvement in HIF-1α inhibition by BP-1T, p53 was knockdown in A549 cells and efficiency was evaluated in immunoblot analysis. The p53 knockout cells were treated in presence of CoCl$_2$ either with or without BP-1T. The results displayed that in the absence of p53, HIF-1α was accumulated and MDM2 level was downregulated (Fig. 5b). The p53 induction by BP-1T without CoCl$_2$ hypoxic condition validated in A549 cells postulates the significant role of BP-1T on p53 expression (Supplementary Fig. 4A), which also reflected in significant level of apoptosis in p53 WT-expressing cells not in p53 silenced or mutant cells (Supplementary Fig. 5A-D). Involvement of p53/MDM2-mediated proteasomal degradation of HIF-1α by BP-1T was reconfirmed by treating the cells with or without MG132 where HIF-1α degradation was reversed in the presence of MG132 (Fig. 5c) which validates involvement of MDM2 on ubiquitination of HIF-1α. MDM2 expression quantified in SCC-9 (p53 mutant) cells evaluated that although MDM2 is higher, HIF-1α
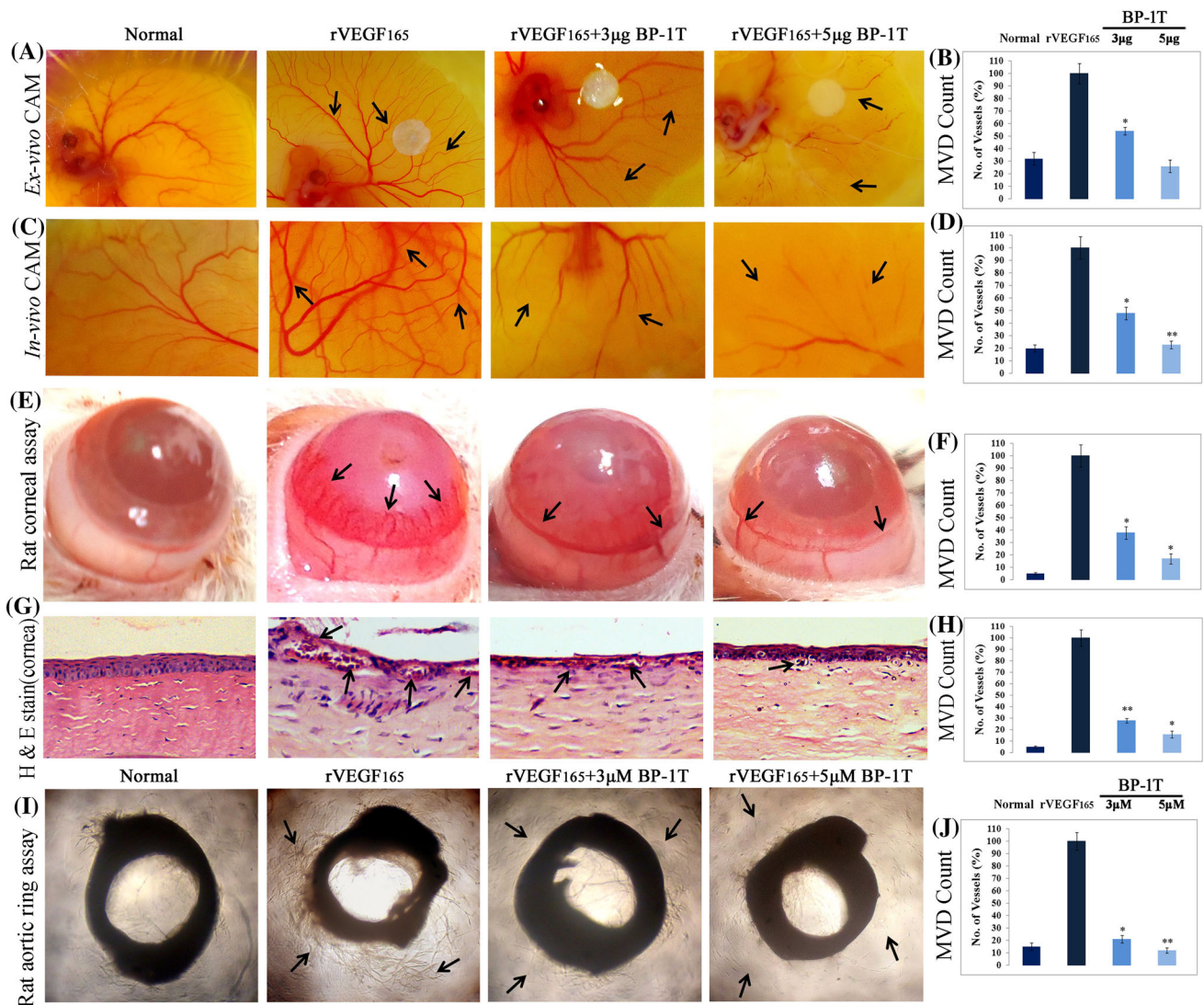
Fig. 2 BP-1T antagonizes the microvascular formation in non-tumour angiogenic models. The effect of BP-1T on neovascularization was studied by stimulating the angiogenesis with rVEGF$_{165}$ and treating with BP-1T at 3 and 5 µg in non-tumour models. **a** Ex vivo and **c** In vivo CAM photographs represent the inhibition of neovessel formation. **b** and **d** Depreciation of MVD. **e** Modulation of sprouting neovessel formation in cornea. **f** Decrease of total corneal vessel length. **g** H&E staining shows reticence of MVD/HPF. **h** Repression of corneal vascular density: To revalidate BP-1T anti-angiogenic efficacy on endothelial cells, rat aortic ring assay was performed. **i** Prohibition of sprouting neovasculature in aortas. **j** Reduction of aortic MVD. Statistical significant values were expressed as *$p < 0.05$ and **$p < 0.01$

proteasomal degradation is p53-dependent (Supplementary Fig. 6A). Cell fractionation studies further authenticated that BP-1T inhibits nuclear accumulation of HIF-1α (Fig. 5d). Together, these results indicate that BP-1T might promote HIF-1α proteasomal degradation through the activation of p53/MDM2 ubiquitination pathway.

BP-1T counteracts the HIF-1α targeted genes

Inhibition of HIF-1α and nuclear accumulation by BP-1T lead to downregulation of HIF-1α-dependent genes in A549 cells such as MMP-2 and MMP-9 as studied by gelatin zymogram and immunoblot analysis, VEGF-A, Flt-1 expression as verified by immunoblots and 3.4- to 5.8-fold reduced secretion of VEGF-A as assessed by ELISA, in a concentration-dependant manner (Fig. 6a–c). As a consequence, sequential pathophysiological process leading to angiogenesis was significantly altered as observed in migration and invasion assays. BP-1T treatment decreases the cancer cell migration up to 79.7 and 85.5 % (Fig. 6d, e), eventually impairing the invasiveness of A549 cells with 82.8 and 87.3 %, when untreated showed maximum migration and invasion (Fig. 6f, g). But no MMP-2 and MMP-9 expressional alteration was found in SCC-9 cells (Supplementary Fig. 6A). These collections of results suggested the repression of HIF-1α by BP-1T cause the inhibition of downstream angiogenic genes.
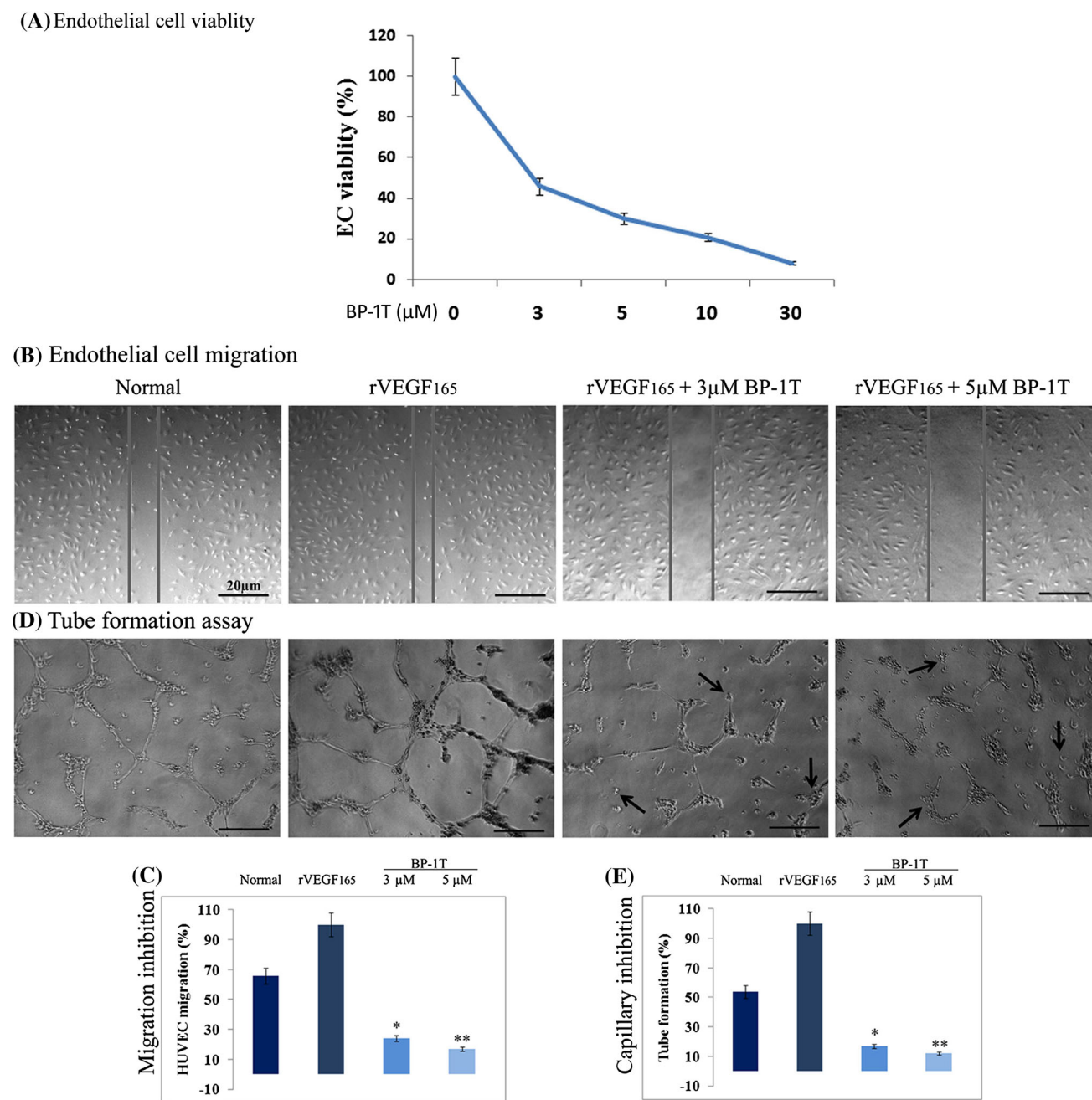
(A) Endothelial cell viablity

(B) Endothelial cell migration

Normal　　　　　rVEGF165　　　rVEGF165 + 3μM BP-1T　　rVEGF165 + 5μM BP-1T

(D) Tube formation assay

(C)

(E)

Fig. 3 BP-1T counteracts the HUVECs migration and capillary tube formations. The potency of BP-1T on HUVECs was studied by viability, migration and tube formation assays through stimulating the HUVECs with rVEGF$_{165}$ and treating with BP-1T. **a** Decrease of endothelial cell viability. **b** Inhibition of endothelial cell migration. **c** Graphical representation of HUVEC migration reduction. **d** Regression of capillary tube formation. **e** Pictographical illustration of HUVECs tube formation inhibition. Statistical significant values were expressed as *$p < 0.05$ and **$p < 0.01$

BP-1T regresses solid tumour progression targeting angiogenesis in vivo

Solid tumour model is most reliable model for angiogenesis studies, and Dalton's lymphoma (DL) cells were used to develop solid tumour (DLS) [20, 32]. After onset of tumour development up to 100 mm^3 size, 6 doses of BP-1T at 30 and 50 mg/kg (*b.w*) on every alternate days reduced the tumour growth in dose-dependent manner with notable reduction in physical morphology of tumour-bearing animals as measured by vernier caliper (Fig. 7a, b). The dissected tumour size depicted the tumour regression with 2.57- to 4.5-folds inhibition (Fig. 7c, d) which resulted in >2.3-fold increased survivability (Fig. 7e). BP-1T is
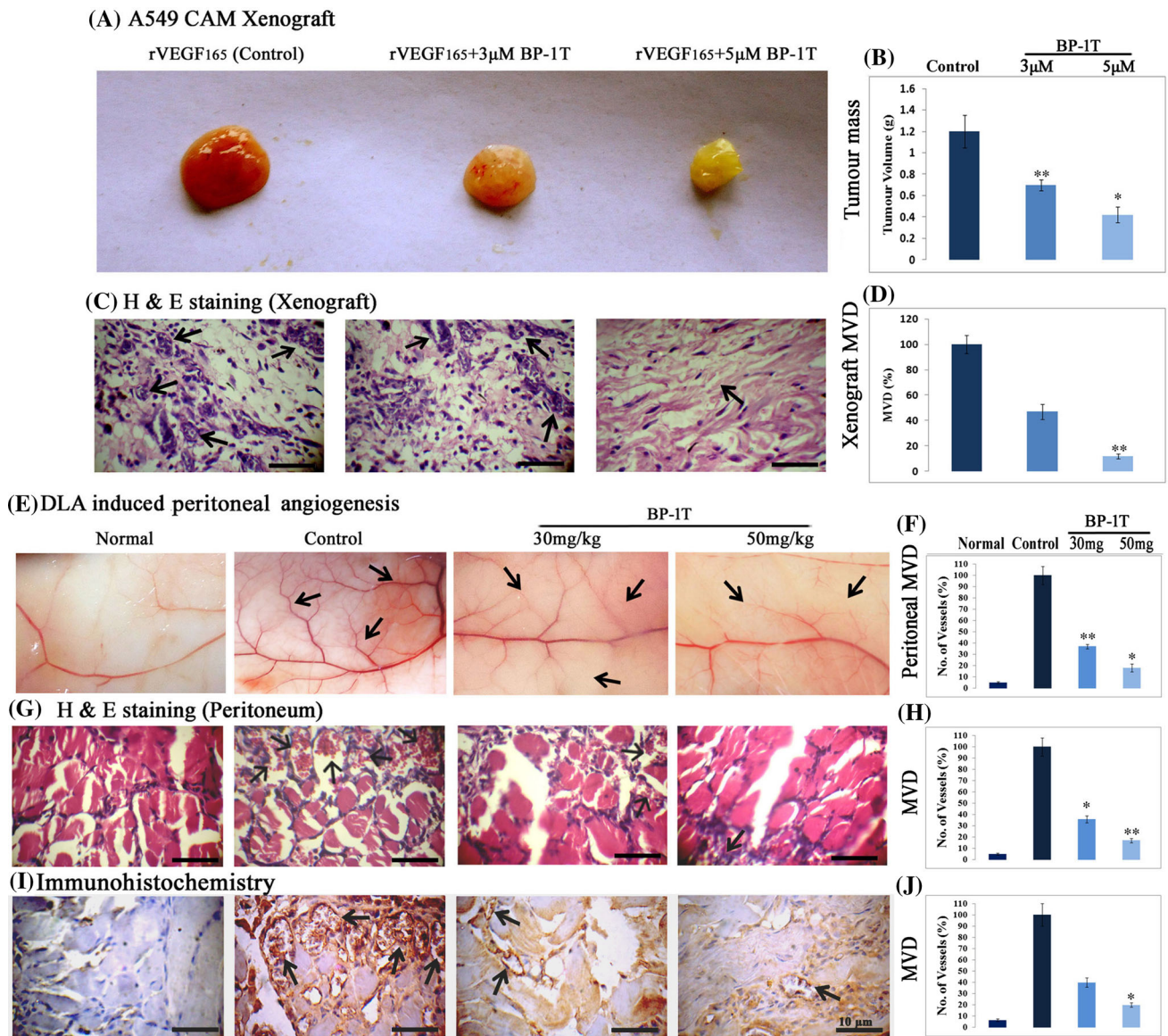
Fig. 4 BP-1T inhibits the neovascularization in tumour angiogenic models. To validate angiopreventive effect of BP-1T on tumour-induced angiogenesis, ECM gel containing A549 cells were cultured in growing CAM embryo with rVEGF₁₆₅, treated with or without BP-1T and incubated for 6 days and tumour parameters, MVD were evaluated. **a** Reduction of tumour growth in A549 xenograft. **b** Regression of tumour mass. **c** H&E stain represents the repression of MVD/HPF. **d** Percentage of A549 tumour MVD inhibition: To re-evaluate the anti-angiogenic effect of BP-1T, peritoneal angiogenesis was induced by culturing DLA cells in mice and administered with BP-1T at 30 mg/kg and 50 mg/kg *b.w* (i.p) for three doses on alternate days, After 3rd dose, effect of BP-1T on peritoneal angiogenesis assessed by H&E stain and IHC. **e** BP-1T antagonized neovascularization of tumour-induced peritoneum. **f** Reduction of neovessel length. **g** and **i** Pictographic representation of reduction of vascular density (MVD/HPF). **h** and **j** Graphical representation of percentage of MVD inhibition. Statistical significant values were expressed as *$p < 0.05$ and **$p < 0.01$

known for the less or no toxic effects [21] which was re-assessed in liver and spleen morphology and histological studies, illustrating no significant changes (Supplementary Fig. 7A–D). Regression of the tumour volume counter-acted with reduced neovascular density with MVD/HPF of 10.4 ± 2.4 and 5.7 ± 1.2 compared to 21.6 ± 2.8 of control as verified by histopathological and IHC analysis (Fig. 8a–d).

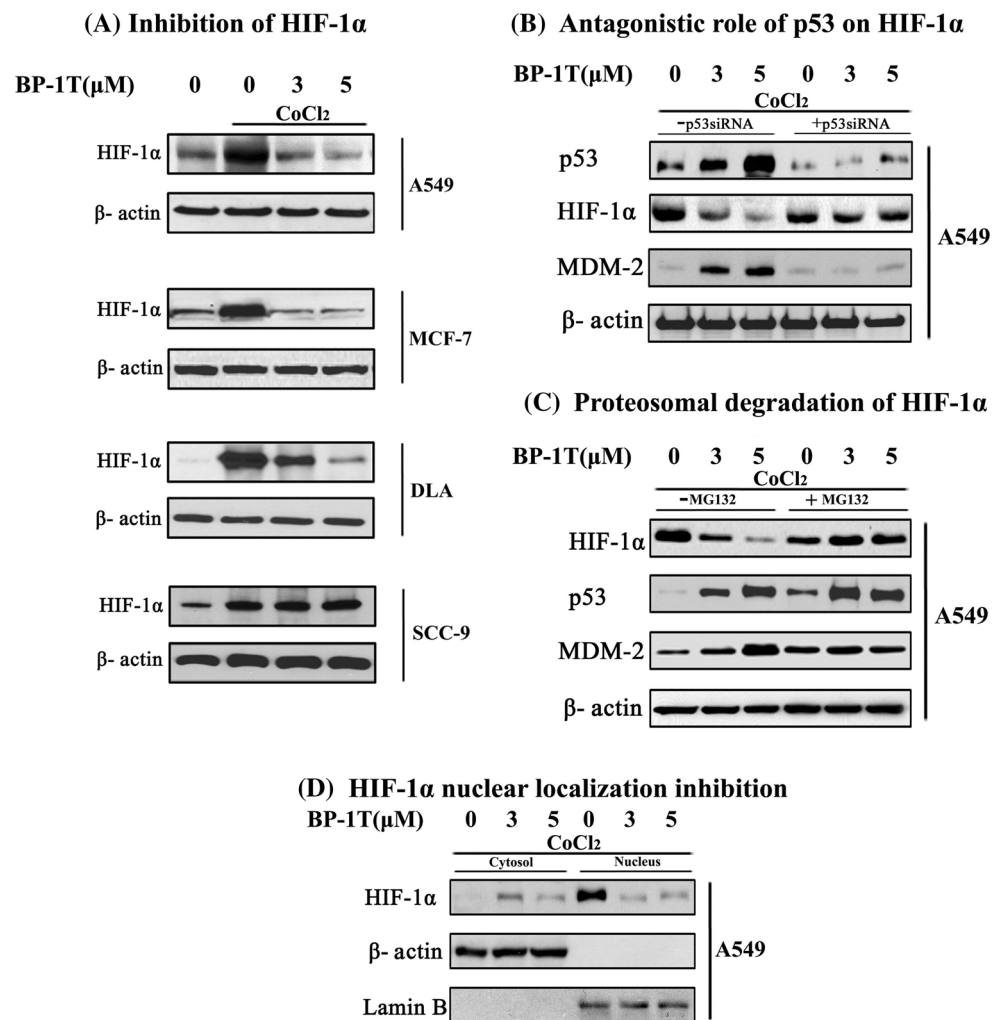## BP-1T inhibits the HIF-1α signalling in hypoxic solid tumour in vivo

The effect of BP-1T on in vitro studies was re-evaluated in in vivo HIF-1α signalling in hypoxic solid tumour (DLS). BP-1T is not affecting the mRNA expression of HIF-1α as studied by semi-quantitative-PCR (Fig. 9a) but negatively regulated HIF-1α protein accumulation by immunoblot and IHC in

Fig. 5 BP-1T targets the HIF-1α signalling through the activation of p53/MDM2 pathway. The effect of BP-1T (0, 3, 5 μM) on HIF-1α expressions against various cancer cell lines (A549, MCF-7, DLA and SCC-9) under the condition of normoxia and CoCl₂-induced hypoxia condition was determined by immunoblot analysis. **a** Inhibition of HIF-1α expression in A549, MCF-7 and DLA cells and no alteration in SCC-9 cells: The role of p53 in BP-1T induced HIF-1α inhibition was determined by siRNA approach. **b** Deterioration of HIF-1α expression through p53 and MDM2 expression: The effect of BP-1T on the stability of HIF-1α was examined in A549 cells pretreated with or without MG132 and treated with BP-1T for 48 h. **c** Ubiquitination of HIF-1α through activation of p53 and MDM2: Cell fractionation studies were carried out to validate HIF-1α nuclear translocation. **d** Inhibition of nuclear translocation of HIF-1α

(A) Inhibition of HIF-1α

(B) Antagonistic role of p53 on HIF-1α

(C) Proteosomal degradation of HIF-1α

(D) HIF-1α nuclear localization inhibition

concentration-dependent manner (Fig. 9b). Diminished HIF-1α expression is due to overexpression of p53 and MDM2 as illustrated in immunoblot and IHC (Fig. 9b, c). Resulted HIF-1α degradation eventually abrogated its downstream genes such as MMP-2 and MMP-9 as assessed by zymogram, immunoblots and IHC (Fig. 9d–f), VEGF-A, Flt-1 by RT-–PCR, immunoblots (Fig. 9g, h) and serum VEGF-A by ELISA (Fig. 9i) which is concurrent with in vitro results. Altogether, the current study results conclude that BP-1T counteracts HIF-1 signalling through the activation of p53/MDM2-mediated HIF-1α degradation (Fig. 10).

Discussion

Our research is focused in searching new active cytotoxic and target-specific small molecule targeting tumour angiogenesis. In cancer therapy, though a noticeable number of novel anti-neoplastic cytotoxic molecules have

been introduced, they have failed to reach the bedside due to their non-specificity and adverse effects [36]. A design of molecule which overcomes such problems is necessary for considering as a potent cancer inhibitor [37]. Earlier, we have made an effort for designing a benzophenone derivatives with target specific action and subjected them for high-throughput cell-based screening system and revealed there molecular targets [16–20, 38, 39]. BP-1T emerged as putative role in inhibition of tumour angiogenesis in preliminary pilot screening [21]. In current study, we have expanded to validate BP-1T-mediated mechanism.

In a course of drug development process, it is always been suggested to screen against multiple cancer cell line with different origin for better assessment [40]. Drawing such an action BP-1T turned out has persuasive cytotoxic and prolonged effect against various cancer types including A549, MCF-7 and SCC-9 cells (Table 1) (Fig. 1b–f and Supplementary Fig. 1A & B).
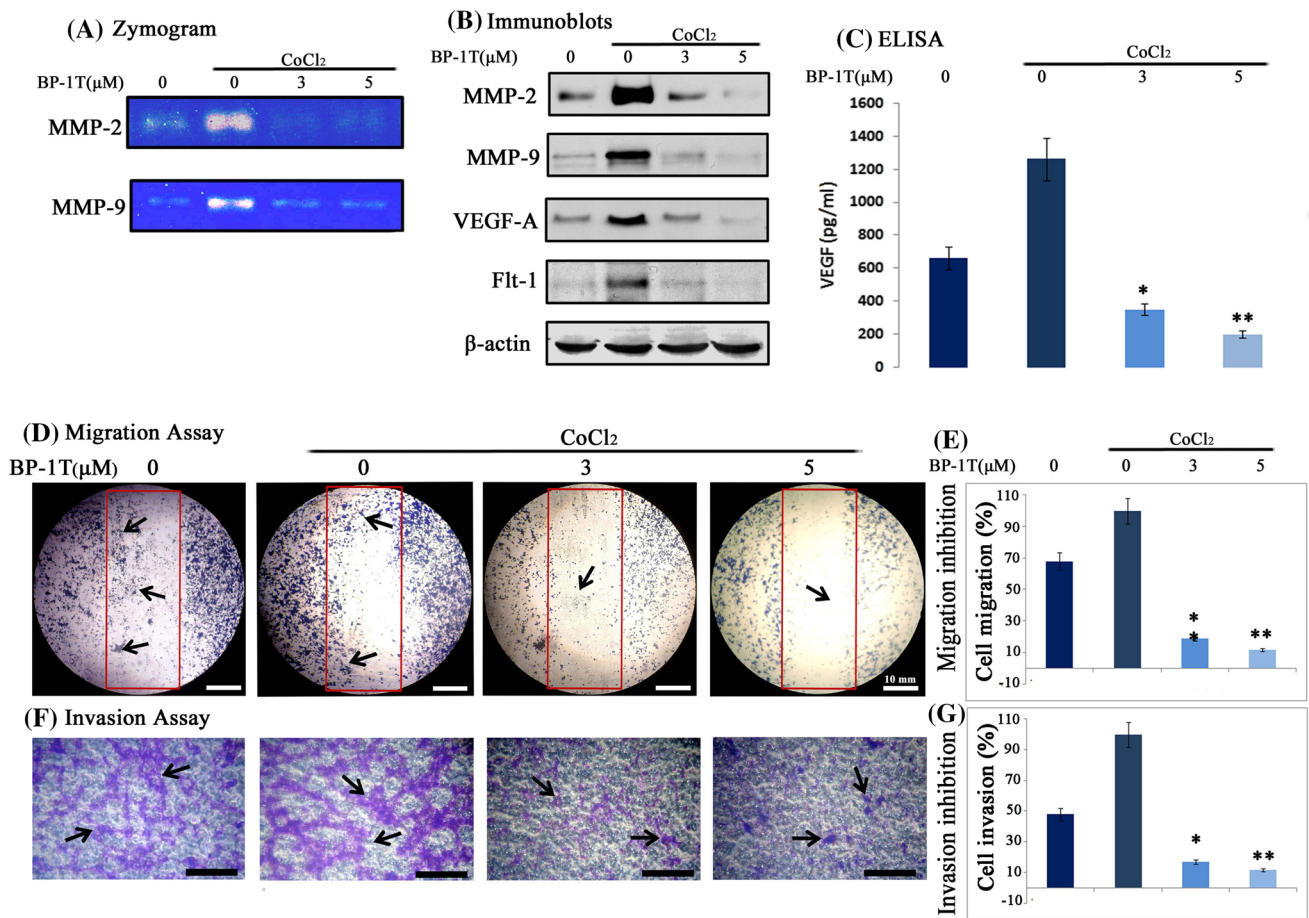
Fig. 6 BP-1T inhibits HIF-1α-dependent downstream gene expressions and cell migration and invasion of A549 cells. Conditioned media and lysates were prepared from A549 cells treated with BP-1T (0, 3, 5 μM) and subjected to gelatin zymogram and immunoblot analysis. **a** Decrease of gelatinase activity of MMP-2 and MMP-9. **b** Suppression of MMP-2 and MMP-9, VEGF-A and Flt-1 gene expression. **c** Inhibition of VEGF-A secretion. Monolayer of A549 cells scratched to form wound and treated with BP-1T for 48 h to evaluate the effect of BP-1T on migration. **d** Inhibition of A549 cell migration. **e** Percentage of migration inhibition. The effect of BP-1T on invasion was assessed by Matrigel transwell invasion assay. **f** Inhibition of invasion of A549 cells. **g** Percentage of invasion inhibition. Statistical significant values were expressed as *$p < 0.05$ and **$p < 0.01$

VEGF being a predominant player in induction of angiogenesis is used in reliable non-tumour angiogenesis assay models which is very well authenticated for its target action on neovascularization. [41, 42]. The rVEGF$_{165}$-induced angiogenesis in ex vivo and in vivo CAM assays, rat corneal micropocket and aortic ring assay models was drastically reduced by BP-1T inferring its explicit in action (Fig. 2a–d). The induction of functional endothelial cell death can restrict redundant neovascularization of tumours by altering endothelial cell density, migration and tube remodelling [8, 35, 42–44]. More importantly, BP-1T markedly retarded the human functional endothelial cell migration, adjacent cell linking and capillary tube forming efficiency of HUVECs with irregular/apoptotic cell morphology (Fig. 3b–e) which indicates the apoptogenic and toxic effect of BP-1T on endothelial cell proliferation (Fig. 3a). BP-1T on apoptotic signalling cascade modulation needs further validation.

Tumour angiogenesis is the proliferation of existing blood vessels penetrating into the tumours to supply nutrients, oxygen and is essentially required for the growth and metastasis of solid tumours [43]; therefore, inhibition of microvascular density in tumour is an important aspect in cancer prevention [44, 45]. Studies on xenograft models are crucial in validating the drug potentiality which mimics in vivo physiological environment [27]. Antiangiogenic effect of BP-1T was reproduced in CAM xenograft of human lung adenocarcinoma (A549) tumour model, resulting regressed tumour growth (Fig. 4a–d). To strengthen the results, secreted VEGF of ascites tumour-induced peritoneal angiogenesis [45, 46] in in vivo DLA model was evaluated for BP-1T efficacy resulting in repressed MVD to be more specific in CD31 counts, expressed only on endothelial cells which is diagnostic marker (Fig. 4e–j). As consequences, the tumour growth parameters were also altered which relied on
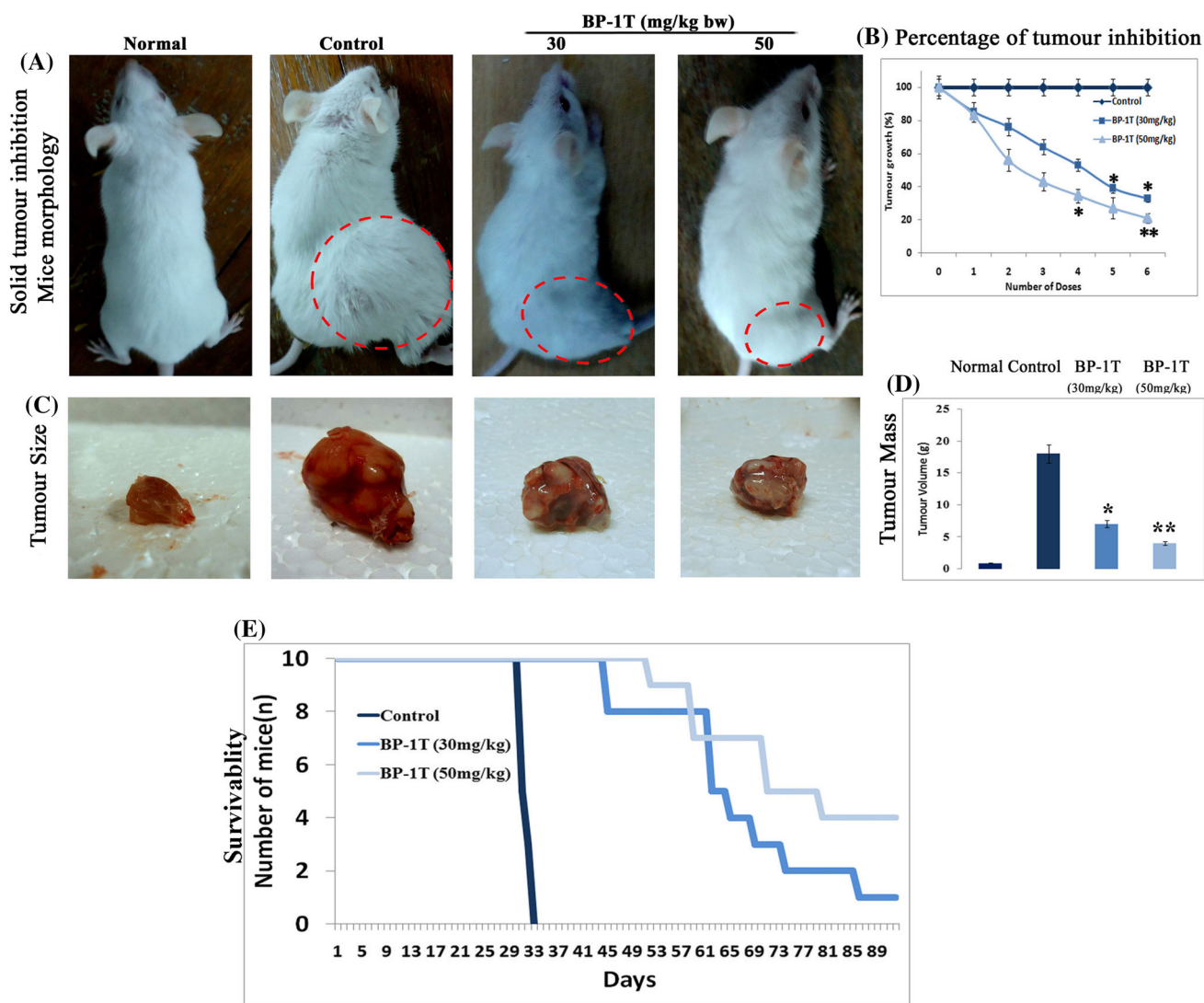
Fig. 7 BP-1T represses the establishment of Dalton's lymphoma solid tumour (DLS) by antagonizing neovasculogenesis. DLA cells (5×10^6 cells/thigh s.c) were injected into the right thigh of the mice to develop solid tumour. Following visible tumour development (100 mm^3), mice were grouped and administered with BP-1T (0, 30, 50 mg/kg *b.w* (i.p), 6 doses). At the end of 35th day (after 6 doses), tumour parameters were noticed and tumour tissues were processed for MVD quantifications. Survivals of DL solid tumour-bearing treated versus untreated animals were noticed. **a** Morphology of mice bearing solid tumour. **b** Percentage of tumour inhibition. **c** Reduction of solid tumour mass. **d** Graphical representation tumour volume. **e** Prolonged survivability. Statistical significant values were expressed as *$p < 0.05$ and **$p < 0.01$

neovascularization. Moreover, BP-1T exhibited no or very negligible adverse effects [21] with no modulation in histopathology of liver and spleen (Supplementary. 7A-D). Collected evidences display that BP-1T has a strong antiangiogenic potentiality.

Pathophysiology of tumour angiogenesis is a consequence of hypoxic microenvironment in solid tumours due to inadequate vascularization which results in poor prognosis and therapeutic resistance due to HIF-1α activation which transcribes set of angiogenic gene [5, 8, 47]. During normal physiological process, existence of normoxic condition regulates HIF-1α expression by prolyl hydroxylating

through hydroxylase (PHD) which is required for pVHL and E3 ubiquitin-mediated proteasomal degradation. But under hypoxia, the absence of oxygen blocks the PHD which facilitates the HIF-1α to escape from pVHL-mediated proteasomal degradation [3–5, 48]. On the other side, half of the tumours types are pVHL mutated which eases the HIF-1α accumulation [49]. Considering the profound impacts of HIF-1α on angiogenesis and cancer progression via microenvironment and unsatisfactory efficacy of targeting pVHL pathway, our research focused on the identification of novel HIF-1α inhibitor which targets the pVHL-independent pathway.
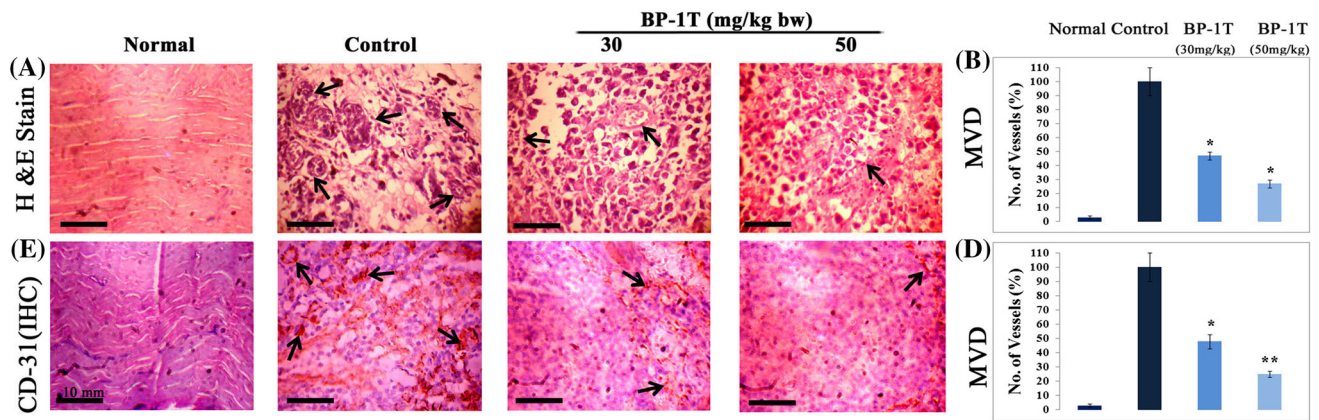
Fig. 8 BP-1T reduces the microvascular density of DLS tumour. BP-1T treated and untreated tumour sections were analysed by histopathology and CD-31 staining. **a** Reduction of neovessel formation. **b** Percentage of MVD inhibition. **c** Decrease of CD-31 endothelial cell marker stain. **d** Percentage of CD-31 expression inhibition. Statistical significant values were expressed as $*p < 0.05$ and $**p < 0.01$

The relationship between HIF-1α, p53 and MDM2 has a pivotal role in the regulation of HIF-1α. In response to hypoxia, HIF-1α is highly expressed and interacts with p53; therefore, HIF-1α stabilizes and protects the p53 from MDM2-mediated degradation [50], but p53 negatively regulates HIF-1α and provides the HIF-1α to MDM2 for ubiquitination process, subsequently HIF-1α gets degraded by proteasome [11–13, 51]. Nevertheless, MDM2 has a negative role in p53 regulation during normal conditions, but it enhances the p53 stabilization by associating with unacetylated HIF-1α during hypoxia and acts as a bridge between HIF-1α and p53 thereby facilitates the ubiquitination of HIF-1α [11–15]. Moreover, loss of p53 (WT) and MDM2 during hypoxia enormously increased the HIF-1α expression and stability in $p53^{-/-}$ and $MDM2^{-/-}$ cells [11, 14, 51]. In our study, CoCl$_2$ was used to mimic hypoxia condition since it blocks the activity of PHD [52], which facilitates cellular HIF-1α accumulation. Results are consistent with experimental observations that BP-1T is found to effectively inhibit the HIF-1α expression in A549, MCF-7 and DLA cells but not in SCC-9 cells (Fig. 5a). Interpreting our results A549, MCF-7 and DLA exhibits wild-type (WT) p53 and mutant p53 in SCC-9 inferring the role of p53 (WT) in BP-1T-mediated HIF-1α inhibition. The silencing of p53 in A549 cells supported our results (Fig. 5b). Since MDM2 involved in p53-mediated ubiquitination of HIF-1α, MDM2 levels were assessed and found that induced MDM2 expression eventually promotes HIF-1α degradation by BP-1T (Fig. 5b, c). Proteasome inhibition assay using MG132 further validated the results. In the absence of MG132, BP-1T promotes the proteasomal degradation of HIF-1α through the mediation of p53/MDM2 but is reversible in the presence of MG132 (Fig. 5c).

While induction of p53 will occur only during severe hypoxia (very low O$_2$) or anoxia conditions [53], but BP-1T treatment was able to induce p53 in normoxia (Supplementary Fig. 4 or CoCl$_2$ conditions (Fig. 5b). This result authenticates the activity of BP-1T on p53 induction and stabilization. There are several reports highlighting the overexpression of p53 (WT) decreases the HIF-1α but not with mutant p53 in both in vitro and in vivo [54–56]. The p53 and MDM2 interaction causes the loss of p53 [56]. However, our data show that BP-1T mediates accumulation of both p53 and MDM2 (Fig. 5b, c) which indicates that BP-1T blocks the p53–MDM2 interaction which leads to HIF-1α downregulation. HIF-1α is targeted by proteasome mediation through either VHL or p53/MDM2 pathway, but our experimental data show that HIF-1α is regulated by proteasome-dependent manner (Fig. 5c) when CoCl$_2$ is used for blocking VHL pathway. This effect validates the ubiquitinating activity of MDM2 on HIF-1α stabilization with support of p53 (Fig. 5c), and also MDM2 expression was found significantly in SCC-9 (p53 mutant) cells (Supplementary Fig. 6) where HIF-1α is not altered (Fig. 5a), which makes clear that p53/MDM2 involvement in HIF-1α proteasomal degradation. Since p53 has a critical role in apoptosis, induction of p53 by BP-1T (Supplementary Fig. 4A) leads to considerable apoptotic cell death (not in BP-1T untreated) in p53 WT-expressing cells but not in p53 silenced or mutant cells (Supplementary Fig. 5A-D).

Nuclear HIF-1α accumulations mediate the transcriptional activation of VEGF-A, Flt-1, MMP-2 and MMP-9 expressions which plays an important role in the formation of novel blood vessels and metastasis [3, 5, 57]. Inhibition of HIF-1α expression by BP-1T eventually leads to abridged nuclear translocation of HIF-1α (Fig. 5d),
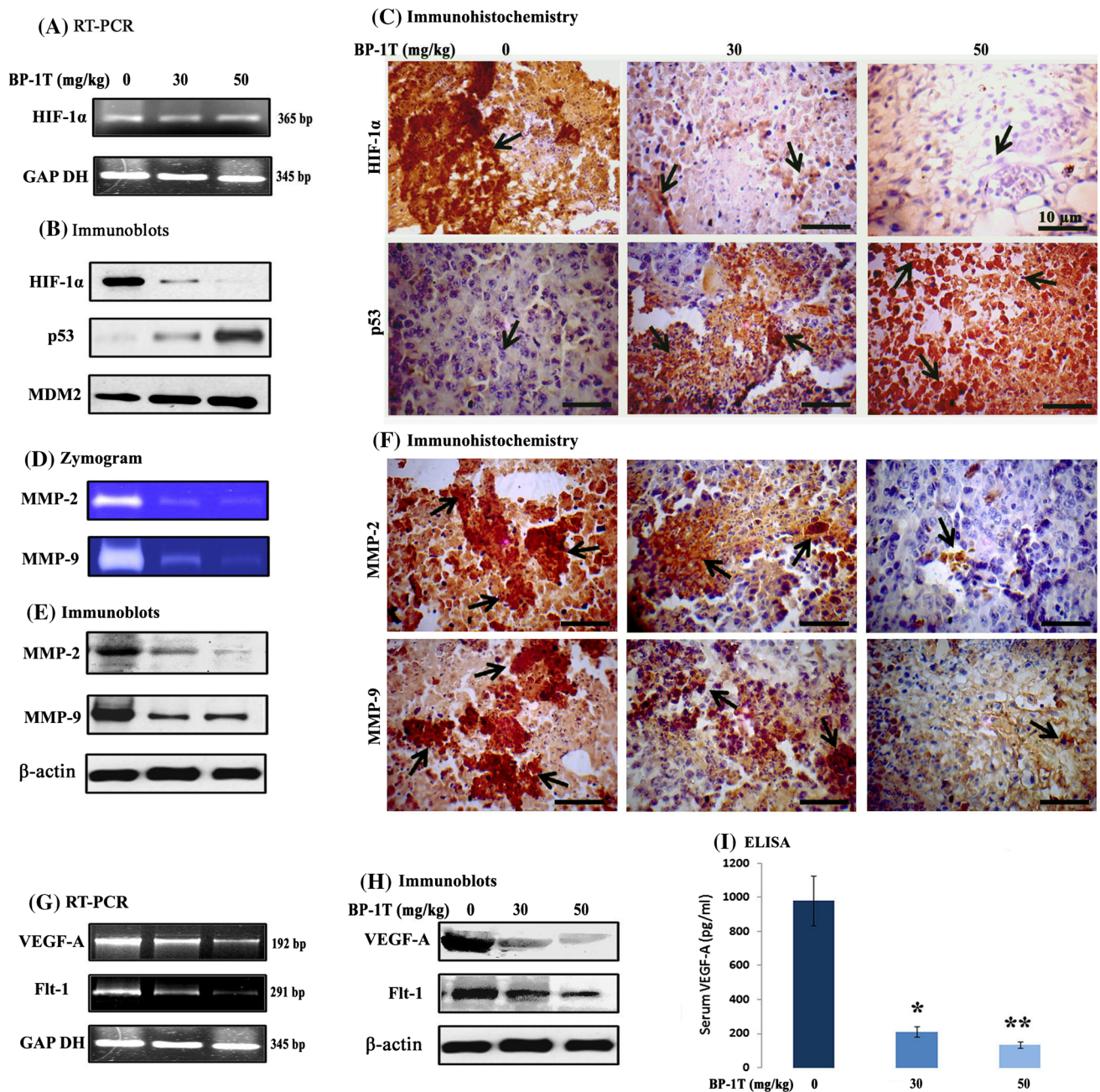
Fig. 9 BP-1T regresses the HIF-1α target gene expression by targeting accumulation of HIF-1α in DLS. Total RNA, whole-cell lysates, tissue sections were prepared from tissues of DLS of control and BP-1T treated groups. RT-PCR (30 cycles), gelatin zymogram and immunoblots were carried out. **a** No transcriptional alteration of HIF-1α expression. **b** Inhibition of translational HIF-1α through the activation of p53 and MDM2 expressions. **c** Decrease of HIF-1α

accumulation through the stimulation of p53 expression. **d** Reduction of gelatinase activity of MMP-2 and MMP-9. **e** and **f** Regression of MMP-2 and MMP-9 expression. **g** and **h** Repression of transcriptional and translational expression of VEGF-A and Flt-1. **i** Reduction of serum VEGF-A. Statistical significant values were expressed as *$p < 0.05$ and **$p < 0.01$

resulting in altered expression of downstream target genes such as MMP-2 and MMP-9, VEGF-A and Flt-1 in in vitro (Fig. 6a–c). Nevertheless, SCC-9 (p53 mutant) exhibited no alteration in downstream target genes of HIF-1α (Supplementary Fig. 6A). MMPs play an important role in degradation of extracellular matrix leading to migration

and invasion of tumour cells [58]. BP-1T intermediates this process thereby completely blocking the process of angiogenesis (Fig. 6d–g).

Validation of in vitro results is crucial only when results were able reproduced in in vivo physiological system and is an important step in pharmacophore development.
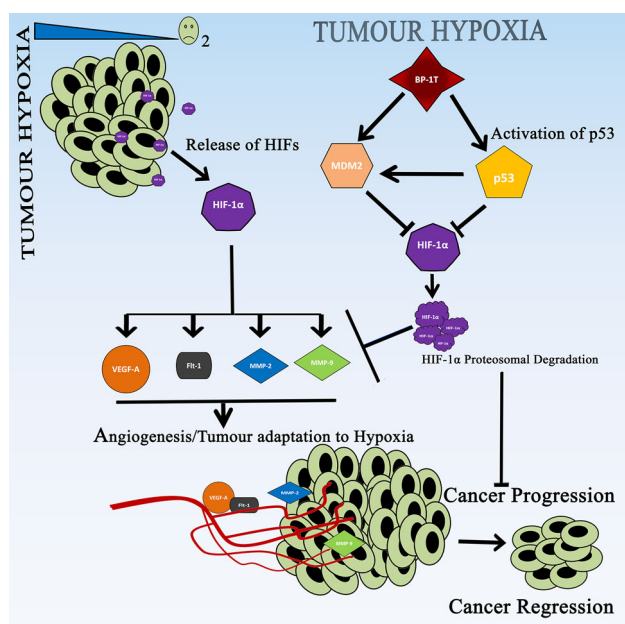
Fig. 10 Schematic representation of BP-1T effect on tumour hypoxia induced signalling

Hypoxia is best characterized as an HIF activator. When intensively proliferating cells form a solid tumour, the balance between oxygen supply and demand is impaired; consequently, microenvironment, (intratumoural hypoxia) prevailed in growing cell masses to facilitate the tumour neovasculature [35, 43]. In vivo solid tumour microenvironment is purely hypoxic in nature and suitable model for antiangiogenic drug development process [31, 43, 59]. BP-1T treatment induces the expression of p53 and MDM2, by which targets the HIF-1α for proteasomal degradation (Fig. 9a–c), which is synchronized with in vitro results (Fig. 5a–c). Further findings on HIF-1α downstream signalling concluded that BP-1T downregulates the VEGF-A, Flt-1, MMP-2 and MMP-9 which are predominant in tumour angiogenesis (Fig. 9d–i). The inhibition of angiogenesis (MVD) (Fig. 8a–d) by BP-1T resulted in the reduction of tumour progression and extended survivalism in solid tumour model (Fig. 7a–e).

By considering the above observations and results, this present investigation involving in vitro and in vivo experimentations of BP-1T on hypoxia provides strong evidences that BP-1T enhances HIF-1α proteasomal degradation by activating p53/MDM2 ubiquitination pathway and thereby subsequently downregulating the angiogenic genes (Fig. 10), by which BP-1T inhibits the cancer cell proliferation which could be developed as a small molecule inhibitor for cancer therapeutics.

Compliance with ethical standards

Conflict of interest The authors declare that there are no conflicts of interest.

References

1. Cameliet P, Jain RK (2000) Angiogenesis in cancer and other disease. Nature 407(6801):249–257. doi:10.1038/35025220
2. Wang GL, Jiang BH, Rue EA, Semenza GL (1995) Hypoxia inducible factor 1 is a basic-helix-loop-helix-PAS heterodimer regulated by cellular O_2 tension. Proc Natl Acad Sci USA 92(12):5510–5514. http://www.pnas.org/content/92/12/5510.long
3. Xia Y, Choi HK, Lee K (2012) Recent advances in hypoxia-inducible factor (HIF)-1 inhibitors. Eur J Med Chem 49:24–40. doi:10.1016/j.ejmech.2012.01.033
4. Dayan F, Mazure NM, Brahimi-Horn MC, Pouysségur J (2008) A dialogue between the hypoxia-inducible factor and the tumor microenvironment. Cancer Microenviron 1(1):53–68. doi:10.1007/s12307-008-0006-3
5. Semenza GL (2003) Targeting HIF1 for cancer therapy. Nat Rev Cancer 3(10):721–732. doi:10.1038/nrc1187
6. Hong SS, Lee H, Kim KW (2004) HIF-1α: a valid therapeutic target for tumor therapy. Cancer Res Treat 36(6):343–353. doi:10.4143/crt.2004.36.6.343
7. Forsythe JA, Jiang BH, Iyer NV, Agani F, Leung SW et al (1996) Activation of vascular endothelial growth factor gene transcription by hypoxia-inducible factor 1. Mol Cell Biol 16:4604–4613. doi:10.1128/MCB.16.9.4604
8. Ferrara N, Gerber HP, LeCouter J (2003) The biology of VEGF and its receptors. Nat Med 9:669–676. doi:10.1038/nm0603-669
9. Powis G, Kirkpatrick L (2004) Hypoxia inducible factor-1A as a cancer drug target. Mol Cancer Ther 3(5):647–654. http://mct.aacrjournals.org/content/3/5/647
10. Ke Q, Costa M (2006) Hypoxia-inducible factor-1 (HIF-1). Mol Pharmacol 70(5):1469–1480. doi:10.1124/mol.106.027029
11. Ravi R, Mookerjee B, Bhujwalla ZM, Sutter CH, Artemov D, Zeng Q et al (2000) Regulation of tumor angiogenesis by p53-induced degradation of hypoxia-inducible factor 1alpha. Genes Dev 14(1):34–44. doi:10.1101/gad.14.1.34
12. Zhou CH, Zhang XP, Liu F, Wang W (2015) Modeling the interplay between the HIF-1 and p53 pathways in hypoxia. Sci Rep 5:13834. doi:10.1038/srep13834
13. Amelio I, Inoue S, Markert EK, Levine AJ, Knight RA, Mak TW, Melino G (2015) TAp73 opposes tumor angiogenesis by promoting hypoxia-inducible factor 1α degradation. Proc Natl Acad Sci USA 112(1):226–231. doi:10.1073/pnas.1410609111
14. Joshi S, Singh AR, Durden DL (2014) MDM2 regulates hypoxic hypoxia inducible factor 1α stability in an E3 ligase, proteasome, and PTEN phosphatidyl inositol 3 kinase AKT dependent manner. J Biol Chem 289(33):22785–22797. doi:10.1074/jbc.M114.587493
15. Chen D, Li M, Luo J, Gu W (2003) Direct interactions between HIF-1 alpha and MDM2 modulate p53 function. J Biol Chem 78(16):13595–13598. doi:10.1074/jbc.C200694200

16. Shankar J, Thippegowda PB, Khanum SA (2009) Inhibition of HIF-1a activity by BP-1 ameliorates adjuvant induced arthritis in rats. Biochem Biophys Res Commun 387(2):223–228. doi:10.1016/j.bbrc.2009.01.086

17. Ranganatha VL, Vijay Avin BR, Thirusangu P, Prashanth T, Prabhakar BT, Khanum SA (2013) Synthesis, angiopreventive activity, and in vivo tumor inhibition of novel benzophenone–benzimidazole analogs. Life Sci 93(23):904–911. doi:10.1016/j.lfs.2013.10.001

18. Prabhakar BT, Khanum SA, Jayashree K, Salimath BP, Shashikanth S (2006) Antitumor and proapoptotic effect of novel synthetic benzophenone analogues in Ehrlich ascites tumor cells. Bioorg Med Chem 14(2):435–446. doi:10.1016/j.bmc.2005.08.039

19. Prabhakar BT, KhanumSA SS, Salimath BP (2006) Antiangiogenic effect of 2-benzoylphenoxy acetamide in EAT cell is mediated by HIF-1α and down regulation of VEGF of in-vivo. Invest N Drugs 24(6):471–478. doi:10.1007/s10637-006-6587-0

20. Vijay Avin BR, Thirusangu P, Ranganatha VL, Firdouse A, Prabhakar BT, Khanum SA (2014) Synthesis and tumor inhibitory activity of novel coumarin analogs targeting angiogenesis and apoptosis. Eur J Med Chem 75:211–221. doi:10.1016/j.ejmech.2014.01.050

21. Prashanth T, Thirusangu P, Vijay Avin BR, Ranganatha VL, Prabhakar BT, Khanum SA (2014) Synthesis and evaluation of novel benzophenone-thiazole derivatives as potent VEGF-A inhibitors. Eur J Med Chem 87:274–283. doi:10.1016/j.ejmech.2014.09.069

22. Xu LF, Ni JY, Sun HL, Chen YT, Wu YD (2013) Effects of hypoxia-inducible factor-1α silencing on the proliferation of CBRH-7919 hepatoma cells. World J Gastroenterol 19(11):1749–1759. doi:10.3748/wjg.v19.i11.1749

23. Bair AM, Thippegowda PB, Freichel M, Cheng N, Ye RD, Vogel SM, Yu Y, Flockerzi V, Malik AB, Tiruppathi C (2009) Ca2+ entry via TRPC channels is necessary for thrombin-induced NF-kappaB activation in endothelial cells through AMP-activated protein kinase and protein kinase Cdelta. J Biol Chem 284(1):563–574. doi:10.1074/jbc.M803984200

24. Franken NA, Rodermond HM, Stap J, Haveman J, van Bree C (2006) Clonogenic assay of cells in vitro. Nat Protoc 1(5):2315–2319. doi:10.1038/nprot.2006.339

25. Cory G (2011) Scratch-wound assay. Methods Mol Biol 769:25–30. doi:10.1007/978-1-61779-207-6_2

26. Tolboom TC, Huizinga TW (2007) In vitro matrigel fibroblast invasion assay. Methods Mol Med 135:413–421. doi:10.1007/978-1-59745-401-8_27

27. Sys GM, Lapeire L, Stevens N, Favoreel H, Forsyth R, Bracke M, De Wever O (2013) The in ovo CAM-assay as a xenograft model for sarcoma. J Vis Exp 17(77):e50522. doi:10.3791/50522

28. Olfa KZ, Jose L, Salma D, Amine B, Najet SA, Nicolas A et al (2005) Lebestatin, a disintegrin from Macrovipera venom, inhibits integrin-mediated cell adhesion, migration and angiogenesis. Lab Investig 85(12):1507–1516. doi:10.1038/labinvest.3700350

29. Rogers MS, Birsner AE, D'Amato RJ (2007) The mouse cornea micropocket angiogenesis assay. Nat Protoc 2(10):2545–2550. doi:10.1038/nprot.2007.368

30. Kruger EA, Duray PH, Tsokos MG et al (2000) Endostatin inhibits microvessel formation in the ex vivo rat aortic ring angiogenesis assay. Biochem Biophys Res Commun 268(1):183–191. doi:10.1006/bbrc.1999.2018

31. Vijay Avin BR, Prabhu T, Ramesh CK, Vigneshwaran V, Riaz M, Jayashree K, Prabhakar BT (2014) New role of lupeol in reticence of angiogenesis, the cellular parameter of neoplastic progression in tumorigenesis models through altered gene expression. Biochem Biophys Res Commun 448(2):139–144. doi:10.1016/j.bbrc.2014.04.090

32. Hegde M, Karki SS, Thomas E, Kumar S, Panjamurthy K, Ranganatha SR, Rangappa KS, Choudhary B, Raghavan SC (2012) Novel levamisole derivative induces extrinsic pathway of apoptosis in cancer cells and inhibits tumor progression in mice. PLoS One 7(9):e43632. doi:10.1371/journal.pone.0043632

33. Zheng Y, Ni Y, Huang X, Wang Z, Han W (2013) Overexpression of HIF-1α indicates a poor prognosis in tongue carcinoma and may be associated with tumour metastasis. Oncol Lett 5(4):1285–1289. doi:10.3892/ol.2013.1185

34. Jayasooriya RG, Lee YG, Kang CH, Lee KT, Choi YH, Park SY, Hwang JK, Kim GY (2013) Piceatannol inhibits MMP-9-dependent invasion of tumor necrosis factor-α-stimulated DU145 cells by suppressing the Akt-mediated nuclear factor-κB pathway. Oncol Lett 5(1):341–347. doi:10.3892/ol.2012.968

35. Brown JM, Giaccia AJ (1998) The unique physiology of solid tumours: opportunities (and problems) for cancer therapy. Cancer Res 58(7):1408–1416. http://cancerres.aacrjournals.org/content/58/7/1408

36. Singh RP, Agarwal R (2004) A cancer chemopreventive agent silibinin, targets mitogenic and survival signaling in prostate cancer. Mutat Res 555(1–2):21–32. doi:10.1016/j.mrfmmm.2004.05.017

37. De Castro G, Jr AA (2006) Side effects of anti-cancer molecular-targeted therapies (not monoclonal antibodies. Curr Opin Oncol 18(4):307–315. doi:10.1097/01.cco.0000228733.55132.ea

38. Gurupadaswamy HD, Thirusangu P, Vijay Avin BR, Vigneshwaran V et al (2014) DAO-9 (2,5-di(4-aryloylaryloxymethyl)-1,3,4-oxadiazole) exhibits p53 induced apoptogenesis through caspase-3 mediated endonuclease activity in murine carcinoma. Biomed Pharmacother 68(6):791–797. doi:10.1016/j.biopha.2014.07.004

39. Al-Ghorbani M, Thirusangu P, Gurupadaswamy HD, Girish V, Neralagundi HGS, Prabhakar BT, Khanum SA (2016) Synthesis and antiproliferative activity of benzophenone tagged pyridine analogues towards activation of caspase activated DNase mediated nuclear fragmentation in Dalton's lymphoma. Bioorg Chem 65:73–81. doi:10.1016/j.bioorg.2016.02.001

40. Johnston RL, Wockner L, McCart Reed AE, Wiegmans A, Chenevix-Trench G et al (2016) High content screening application for cell-type specific behaviour in heterogeneous primary breast epithelial subpopulations. Breast Cancer Res 18(1):18. doi:10.1186/s13058-016-0681-9

41. Jubb AM, Harris AL (2010) Biomarkers to predict the clinical efficacy of bevacizumab in cancer. Lancet Oncol 11(12):1172–1183. doi:10.1016/S1470-2045(10)70232-1

42. Ferrara N (2002) VEGF and the quest for tumour angiogenesis factors. Nat Rev Cancer 2(10):795–803. doi:10.1038/nrc909

43. Folkman J (1972) Anti-angiogenesis: new concept for therapy of solid tumors. Ann Surg 175(3):409–416

44. Bhat TA, Singh RP (2008) Tumor angiogenesis—a potential target in cancer chemoprevention. Food Chem Toxicol 46(4):1334–1345. doi:10.1016/j.fct.2007.08.032

45. Al-Ghorbani M, Vigneshwaran V, Ranganatha VL, Prabhakar BT, Khanum SA (2015) Synthesis of oxadiazole–morpholine derivatives and manifestation of the repressed CD31 microvessel density (MVD) as tumoral angiogenic parameters in Dalton's Lymphoma. Bioorg Chem 60:136–146. doi:10.1016/j.bioorg.2015.04.008

46. Talmadge JE, Singh RK, Fidler IJ, Raz A (2007) Murine models to evaluate novel and conventional therapeutic strategies for cancer. Am J Pathol 170(3):793–804. doi:10.2353/ajpath.2007.060929

47. Jin Y, Wang H, Liang X, Ma J, Wang Y (2014) Pathological and prognostic significance of hypoxia-inducible factor 1alpha expression in epithelial ovarian cancer: a meta-analysis. Tumour Biol 35(8):8149–8159. doi:10.1007/s13277-014-2059-x

48. Myllyharju J (2013) Prolyl 4-hydroxylases, master regulators of the hypoxia response. Acta Physiol (Oxf) 208(2):148–165. doi:10.1111/apha.12096

49. Bratslavsky G, Sudarshan S, Neckers L, Linehan WM (2007) Pseudohypoxic pathways in renal cell carcinoma. Clin Cancer Res 13(16):4667–4671. doi:10.1158/1078-0432.CCR-06-2510

50. An WG, Kanekal M, Simon MC, Maltepe E, Blagosklonny MV, Neckers LM (1998) Stabilization of wildtype p53 by hypoxia-inducible factor 1α. Nature 392(6674):405–408. doi:10.1038/32925

51. Zhang H, Zhang Z, Xu Y, Xing L, Liu J, Li J, Tan Q (2004) The expression of hypoxia inducible factor 1-alpha in lung cancer and its correlation with p53 and VEGF. J Huazhong Univ Sci Technol Med Sci 24(2):124–127. doi:10.1007/BF02885408

52. Fan L, Li J, Yu Z, Dang X, Wang K (2014) The hypoxia-inducible factor pathway, prolyl hydroxylase domain protein inhibitors, and their roles in bone repair and regeneration. Biomed Res Int 2014:239356. doi:10.1155/2014/239356

53. Schmid T, Zhou J, Brüne B (2004) HIF-1 and p53: communication of transcription factors under hypoxia. J Cell Mol Med 8(4):423–431. doi:10.1111/j.1582-4934.2004.tb00467.x

54. Sermeus A, Michiels C (2011) Reciprocal influence of the p53 and the hypoxic pathways. Cell Death Dis 2:e164. doi:10.1038/cddis.2011.48

55. Brown JM (2007) Tumor hypoxia in cancer therapy. Methods Enzymol 35:297–321. doi:10.1016/S0076-6879(07)35015-5

56. Semenza GL (2013) HIF-1 mediates metabolic responses to intratumoral hypoxia and oncogenic mutations. J Clin Invest 123(9):3664–3671. doi:10.1172/JCI67230

57. Vigneshwaran V, Thirusangu P, Madhusudana S, Krishna V, Pramod SN, Prabhakar BT (2016) The latex sap of the 'Old World Plant' *Lagenaria siceraria* with potent lectin activity mitigates neoplastic malignancy targeting neovasculature and cell death. Int Immunopharmacol 39:158–171. doi:10.1016/j.intimp.2016.07.024

58. Lu P, Takai K, Weaver VM, Werb Z (2011) Extracellular matrix degradation and remodeling in development and disease. Cold Spring Harb Perspect Biol 3(12):1–24. doi:10.1101/cshperspect.a005058

59. Ryan HE, Poloni M, McNulty W et al (2000) Hypoxia-inducible factor-1a is a positive factor in solid tumor growth. Cancer Res 60(15):4010–4015. http://cancerres.aacrjournals.org/content/60/15/4010.long